


## METHODOLOGY

# Flow cytometric quantification of apoptotic and proliferating cells applying an improved method for dissociation of spheroids

Wolfgang Metzger  | Barbara Rösch | Daniela Sossong | Monika Bubel | Tim Pohlemann

Department of Trauma, Hand and Reconstructive Surgery, Saarland University, Homburg, Germany

**Correspondence**

Wolfgang Metzger, Department of Trauma, Hand and Reconstructive Surgery, Saarland University, Bldg 57, 66421 Homburg, Germany.  
Email: johann-wolfgang.metzger@uks.eu

**Abstract**

Spheroids are a promising tool for many cell culture applications, but their microscopic analysis is limited. Flow cytometry on a single cell basis, which requires a gentle but also efficient dissociation of spheroids, could be an alternative analysis. Mono-culture and coculture spheroids consisting of human fibroblasts and human endothelial cells were generated by the liquid overlay technique and were dissociated using AccuMax as a dissociation agent combined with gentle mechanical forces. This study aimed to quantify the number of apoptotic and proliferative cells. We were able to dissociate spheroids of differing size, age, and cellular composition in a single-step dissociation protocol within 10 min. The number of single cells was higher than 95% and in most cases, the viability of the cells after dissociation was higher than 85%. Coculture spheroids exhibited a higher sensitivity as shown by lower viability, higher amount of cellular debris, and a higher amount of apoptotic cells. Considerable expression of the proliferation marker Ki67 could only be seen in 1-day-old spheroids but was already downregulated on Day 3. In summary, our dissociation protocol enabled a fast and gentle dissociation of spheroids for the subsequent flow cytometric analysis. The chosen cell type had a strong influence on cell viability and apoptosis. Initially high rates of proliferative cells decreased rapidly and reached values of healthy tissue 3 days after generation of the spheroids. In conclusion, the flow cytometry of dissociated spheroids could be a promising analytical tool, which could be ideally combined with microscopic techniques.

**KEYWORDS**

activated caspase 3, dissociation, flow cytometry, Ki67, live-dead-assay, spheroids

**Abbreviations:** AO, acridin orange; DMEM, Dulbecco's modified Eagle medium; ECG MV, endothelial cell growth medium MV; ECM, extracellular matrix; HDMEC, human dermal microvascular endothelial cells; LOT, liquid overlay technique; LL, lower left; LR, lower right; NHDF, normal human dermal fibroblasts; PBS, phosphate-buffered saline; PE, phycoerythrin; PI, propidium iodide; UL, upper left; UR, upper right.

This is an open access article under the terms of the Creative Commons Attribution-NonCommercial-NoDerivs License, which permits use and distribution in any medium, provided the original work is properly cited, the use is non-commercial and no modifications or adaptations are made.

© 2021 The Authors. Cell Biology International published by John Wiley & Sons Ltd on behalf of International Federation of Cell Biology.

## 1 | INTRODUCTION

Spheroids are three-dimensional (3D) aggregates of cells, which can be generated from a single cell suspension by different techniques (Achilli et al., 2012) for example, hanging drop technique, liquid overlay technique (LOT), or spinner flasks just to name a few. It is important to know that spheroids do not need any stabilizing additional matrix and that the organization of the cells during spheroid formation represents a self-assembling process.

The arrangement of cells within spheroids or cell aggregates can be explained with the differential adhesion hypothesis, which was firstly proposed by Steinberg already in 1970 (Steinberg, 1970). According to this theory, cells behave like immiscible liquids and their arrangement within the spheroids is governed by surface and interfacial tension aiming to reach an energetically favorable organization. Experimental verification of this hypothesis using two L-cell lines with low and high levels of N-cadherin expression revealed that the cells were initially organized incidentally in the spheroids. Of interest, a separation of the cells could clearly be seen after 24 h: Cells with a high level of N-cadherin expression formed the core of the spheroid and were surrounded by cells with a low level of N-cadherin expression (Foty & Steinberg, 2005).

It is widely accepted that the use of spheroids is more suitable to reflect the physiological situation of cells than traditional two-dimensional (2D)-cell culture approaches (Cesarz & Tamama, 2016). In consequence, comparing cellular functions and cellular physiology in 2D and 3D revealed remarkable differences (Arufe et al., 2009; Laschke et al., 2013; Wang et al., 2009), for example, differing sensitivity against cytostatic drugs (Unger et al., 2014). Therefore, spheroids are a promising preclinical test system, which might help to reduce the high attrition rate of oncology drug candidates by mimicking the complex microenvironment of tumors better than 2D-cell cultures (Lazzari et al., 2018; Meier-Hubberten & Sanderson, 2019). In addition, spheroids have been used in angiogenesis research (Heiss et al., 2015) in the past decades, studies on cell-surface interactions (Metzger et al., 2017), and are highly interesting for tissue engineering applications (Benmeridja et al., 2020).

However, the mentioned benefits of spheroids are countered by a clear limitation in the maximum size of the spheroids. The absence of any vasculature within the spheroids leads to an insufficient supply of oxygen and nutrients as well as an accumulation of metabolic end products. Historically, studies on the physiological situation of cells in spheroids focused on tumor spheroids leading to the widely accepted model of three-layer architecture: Cells in the periphery of tumor spheroids are well supplied and are proliferative. The next layer of cells suffers more and more from under supply and can be defined as GO-rested cells with no proliferative activity. Finally, the supply of the cells in the central region of tumor spheroids is below a critical threshold leading to the development of a necrotic core (Friedrich et al., 2007; Hirschhaeuser et al., 2009). Compared with the physiological situation of cells in tumor spheroids, the number of such studies on nonmalignant spheroids is limited and

some of them draw a different picture. Murphy and coworkers were able to show that in spheroids consisting of mesenchymal stem cells, no hypoxic center and no formation of a necrotic or apoptotic core could be detected even in the case of quite big spheroids consisting of 60,000 cells with a diameter of approximately 700  $\mu\text{m}$  (Murphy et al., 2017).

Due to the 3D architecture, the possibilities of microscopic analysis of spheroids are impaired compared with 2D-cell cultures due to the limited penetration depth of light. Even modern confocal laser scanning microscopy allows only for a penetration depth of 50–80  $\mu\text{m}$  into tissues. Hence, one can reach a higher penetration depth with two-photon laser scanning microscopy (Nimmerjahn et al., 2004) or light-sheet microscopy (Lazzari et al., 2019), but the technical requirements are very high and the needed equipment is cost-intensive and not available in most cell culture labs. To overcome this problem, sectioning of spheroids followed by standard microscopy is one alternative. Even if this approach allows for the advantageous analysis of local distribution patterns throughout the spheroid, considerable time is needed to obtain statistically relevant results (Dorst et al., 2014). In consequence, we favored the dissociation of spheroids into single cells allowing subsequent fluorescence-activated cell sorting (FACS) analysis and could successfully determine the cellular composition of spheroids (Grässer et al., 2018). This success encouraged us to perform the present study, which aimed to further improve our established dissociation protocol and to subsequently quantify the number of dead, apoptotic, and proliferative cells by FACS analysis. We focused on the question, as to which parameter mostly influences the cellular physiology, size or age of the spheroids, or their cellular composition.

## 2 | MATERIALS AND METHODS

### 2.1 | Cell culture and generation of spheroids

Commercially available normal human dermal fibroblasts (NHDF, Lot# 394Z023, PromoCell GmbH) derived from the foreskin of an 8-years old Caucasian boy and human dermal microvascular endothelial cells (HDMEC, Lot# 419Z028.1, PromoCell GmbH) derived from the foreskin of a 6-years old Caucasian boy were expanded as master cell banks according to the manufacturer's instructions up to Passage 4 and stored in liquid nitrogen until usage. Cryo-SFM (PromoCell GmbH) was used as a freezing medium for both types of cells. Standard cell cultivation conditions were chosen (37°C, 95% humidity, 5% CO<sub>2</sub>). NHDF were cultivated in Dulbecco's modified Eagle medium (DMEM, Sigma-Aldrich) with 15% fetal calf serum (PanBiotech) and 1% Penicillin/Streptomycin. HDMECs were cultivated in endothelial cell growth medium MV ([ECG MV], PromoCell GmbH) with 1% Penicillin/Streptomycin. Cells were used in Passages 4 and 5. For detachment with subsequent quantification of the cells, standard trypsinization procedures were applied. The cell number was quantified with the LUNA-FL™ Cell Counter (logos biosystems) in combination with the LUNA™ Cell Counting Slides and the AO/PI

Cell Viability Kit (both logos biosystems) according to the manufacturer's instructions. Each sample was measured in duplicate. The principle of the AO/PI viability kit is the fluorescence staining of living cells with acridine orange (AO) and of dead cells with propidium iodide (PI), which is detected by the LUNA-FL™ cell counter.

Mono-culture spheroids of NHDF and coculture spheroids of NHDF and HDMEC (1:1) were generated by the LOT in the cavities of 96 flat-bottomed well plates (Greiner Bio-One) as previously described in detail (Metzger et al., 2011). In brief, cellular adhesion in the cavities after seeding was prevented by coating with agarose ( $c = 1\%$ , Sigma-Aldrich). In consequence, the cells adhered to each other overnight and formed one spheroid per cavity in a self-organizing process (Metzger et al., 2017). The volume of the cell suspension for each cavity was 100  $\mu\text{l}$  containing 5,000, 10,000, or 50,000 cells, respectively. To exclude any influence of cell culture media on cellular physiology, the same cell culture medium was used for all 3D-cell culture experiments (50% DMEM [15% FCS] and 50% ECG MV with 1% Penicillin/Streptomycin). Spheroids were analyzed and dissociated on Day 1, Day 3, and Day 6 after their generation. Photomicrographs were made with a Nikon Eclipse TS100 phase-contrast microscope (objective 10x/0.25, Ph1 ADL, Nikon Corporation) and a Sony Cybershot 3.0 (Sony Corporation) digital camera. The diameter of spheroids was consecutively measured by analysis of photomicrographs with the ImageJ software (National Institutes of Health).

## 2.2 | Dissociation of spheroids into single cells

The improved method to dissociate spheroids into single cells presented here is based on a protocol, which was already published by our group (Grässer et al., 2018). For each experiment, 200 spheroids (5000 cells), 100 spheroids (10,000 cells), and 30 spheroids (50,000 cells) were harvested with low-retention tips in Falcon tubes. After centrifugation (300g, 4 min), the supernatant was carefully removed, 400  $\mu\text{l}$  AccuMax (Capricorn Scientific GmbH) was added to the spheroids which were then transferred to 1.5 ml reaction tubes. To minimize loss of remaining spheroids, an additional 400  $\mu\text{l}$  AccuMax were added to the Falcon tubes and transferred to the reaction tubes, too. The spheroids were incubated for 10 min at 37°C in a Thermomixer® comfort (Eppendorf) under shaking at 1400 rpm. To support the enzymatic dissociation of spheroids mechanically, the suspension was pipetted 10 times up and down to create shear forces. Here again, low-retention tips were used to minimize cell loss and the tips were slightly pressed against the bottom of the reaction tubes to increase shear forces. Finally, the cell suspension was given on a preseparation filter with a pore size of 70  $\mu\text{m}$  (Miltenyi Biotec), which was filled with 800  $\mu\text{l}$  phosphate-buffered saline (PBS) before. The reaction tubes were rinsed twice with 400  $\mu\text{l}$  PBS and given on the filters, too. The suspension was then passed through the filter into standard tubes for FACS analyses by centrifugation for 4 min at 300g. After the removal of 2000  $\mu\text{l}$  of the supernatant, 600  $\mu\text{l}$  PBS was added resulting in a total volume of 1000  $\mu\text{l}$  of cell suspension

for further analysis. In addition to the determination of the cell number, the LUNA FL Cell Counter was also used to quantify the number of single cells to monitor a complete dissociation of the spheroids. We defined a successful dissociation of the spheroids if more than 95% of single cells were quantified.

## 2.3 | Flow cytometric live-dead-assay and quantification of debris

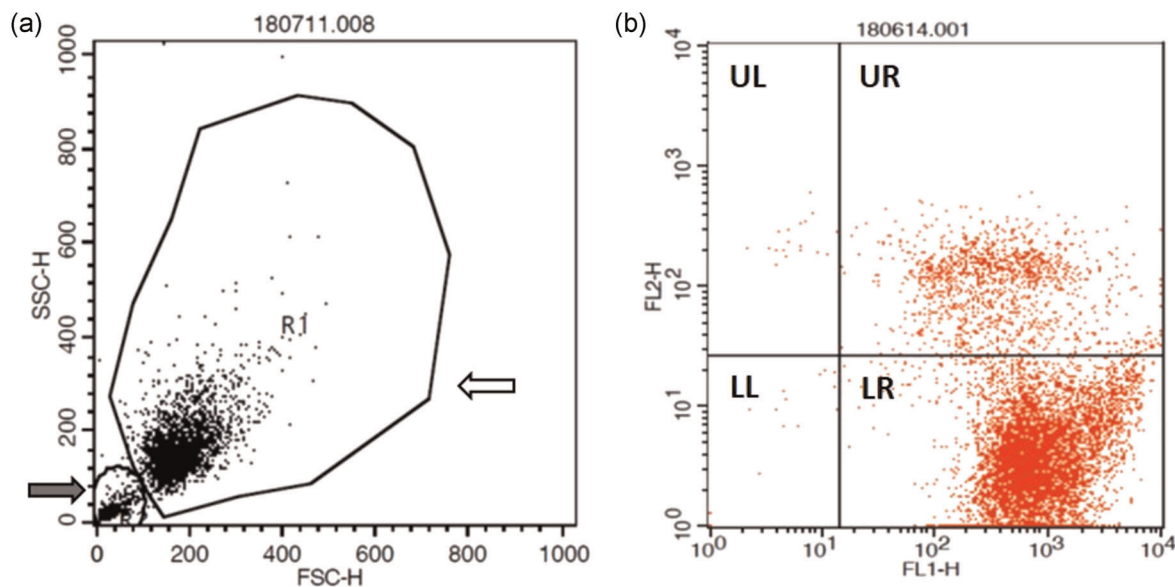
The amount of dead and living cells was quantified flow cytometrically in cell suspensions after dissociation of spheroids. Cells were centrifuged and resuspended in 500  $\mu\text{l}$  PBS. Calcein acetoxymethyl ester (AM) (Cat # C1430, Thermo Fisher Scientific) is commonly used to stain living cells. In living cells, the nonfluorescent calcein AM is hydrolysed by cellular enzymes to form the green fluorescent dye calcein. We prepared a working solution of 50  $\mu\text{M}$  in dimethylsulfoxide (Carl Roth GmbH & Co KG). PI (Cat # P4864,  $c = 1 \text{ mg/ml}$ , Sigma-Aldrich) is a red fluorescent dye that is not able to pass intact membranes of living cells but of dead cells with impaired membrane integrity. After the addition of 2  $\mu\text{l}$  of calcein AM and 1  $\mu\text{l}$  of PI, the cells were incubated for 20 min at room temperature in the dark, washed with PBS, and finally resuspended in 500  $\mu\text{l}$  PBS. Flow cytometric analysis was carried out with a FACScan™ device equipped with the CellQuest software (both BD).

Figure 1a shows a typical side-scatter-forward-scatter dot plot, which additionally allows for the discrimination of cellular debris. A typical dot plot of the analysis of the live-dead-assay is shown in Figure 1b. The PI-positive cells are located in the upper left quadrant (UL), the calcein-AM positive cells are located in the lower right quadrant (LR). Few unstained cells can be found in the lower left quadrant (LL) and cells double-stained for calcein-AM and PI can be seen in the upper right quadrant (UR). Cells in UR and LR were counted as living cells

## 2.4 | Flow cytometric quantification of apoptotic cells

Apoptotic cells were quantified flow cytometrically in cell suspensions after dissociation of spheroids. The used PE Active Caspase-3 Apoptosis Kit (BD, Cat # 550914) contains the Cytofix/Cytoperm™ fixation and permeabilization solution, the Perm/Wash™ Buffer (10 $\times$ ) with saponin and the Phycoerythrin (PE) Rabbit Anti-Active Caspase-3-antibody. A PE Rabbit IgG PE-conjugated antibody (Biotechne, Cat # IC 1051P) was used as isotype control.

After dissociation, the cells were centrifuged for 4 min at 300g, the supernatant was removed and 500  $\mu\text{l}$  of Cytofix/Cytoperm™ fixation and permeabilization solution was added. The cells were incubated for 20 min on ice and were stored overnight at 4°C. Before the antibody staining, the cells were washed twice with Perm/Wash™ Buffer (1 $\times$ ). Dilutions of isotype control antibody ( $c = 1.5 \mu\text{g/ml}$ ) and PE Rabbit Anti-Active Caspase-3-antibody



**FIGURE 1** Typical dot plots illustrating identification of debris and a representative result of a live-dead-assay. (a) Representative SSC-FSC dot plot of a single cell suspension after dissociation of spheroids. R1 shows the population of intact cells (white arrow), the grey arrow indicates the gated cellular debris. (b) Representative dot plot of a single cell suspension after dissociation of spheroids and staining with calcein-AM (FL1) and PI (FL2). The four quadrants show unstained cells (lower left, LL), calcein AM-stained cells (lower right, LR), PI-stained cells (upper left, UL), and double-stained cells (upper right, UR). Cells in UR and LR were defined as living cells; cells in UL were defined as dead cells. AM, calcein acetoxymethylester; PI, propidium iodide; SSC-FSC, side-scatter-forward-scatter

( $c = 1.5 \mu\text{g/ml}$ ) were prepared in Perm/Wash™ Buffer (1x). For each sample and isotype control, 120  $\mu\text{l}$  of antibody solution was added, incubated for 30 min at room temperature, washed and finally re-suspended in 300  $\mu\text{l}$  of Perm/Wash™ Buffer (1x) before flow cytometric analysis with a FACScan™ device equipped with the CellQuest software (both BD).

## 2.5 | Flow cytometric quantification of proliferating cells

Ki67 was chosen as a marker for proliferating cells. After dissociation of spheroids, the cells were centrifuged for 4 min at 300g and 800  $\mu\text{l}$  of the supernatant was removed. For fixation, 500  $\mu\text{l}$  of absolute ethanol ( $-20^\circ\text{C}$ ) was added slowly under continuous movement and the samples were stored for at least 1 h at  $-20^\circ\text{C}$ . Subsequently, the cells were washed with 3 ml of FACS buffer (PBS with 2% FCS), centrifuged again as described above and the supernatant was removed. For staining of Ki67 positive cells, 20  $\mu\text{l}$  of FACS buffer and 2  $\mu\text{l}$  of PerCP-Cy™5.5 Mouse anti-Ki67 antibody (Cat # 550795, BD) or 2  $\mu\text{l}$  of the isotype control PerCP-Cy™5.5 Mouse IgG<sub>1</sub> kappa isotype control (Cat # 561284, BD) was added to each sample, mixed thoroughly and incubated for 30 min in the dark. Finally, FACS buffer ( $V = 1.5 \text{ ml}$ ) was added, centrifuged again and the cells were re-suspended in 0.5 ml of FACS buffer before flow cytometric quantification (FACScan™ equipped with CellQuest Software, both BD).

## 2.6 | Statistical analysis

All results in this study are presented as mean values with standard deviations. Statistical tests were done with the SigmaPlot-Software Version 11.0 (Systat Software Inc.) applying a one-way analysis of variance (ANOVA) or a Kruskal-Wallis one-way ANOVA on Ranks, respectively, if the equal variance test or the test for normally distributed data (Shapiro-Wilk test) was not passed. In both cases, a Student-Newman-Keuls post hoc analysis was done. For the direct comparison of just two groups, a *t* test or a Mann-Whitney Rank Sum Test was run, respectively. If  $p < .05$ , the differences were considered to differ significantly.

## 3 | RESULTS

### 3.1 | Size development of spheroids

As already described earlier (Metzger et al., 2011, 2013), the LOT is both, a powerful and easy technique to generate exactly one spheroid per cavity under highly standardized conditions. The size of the spheroids could easily be determined by adjusting the cellular concentrations in the seeding suspension while keeping the seeding volume of 100  $\mu\text{l}$  per cavity constant (Figure 2). The spheroids exhibited a regular rounded morphology even on Day 1 after generation and almost all seeded cells were integrated in the spheroid. Of note, the morphology of the coculture spheroids was a little bit more irregular in comparison to the mono-culture spheroids. Furthermore,

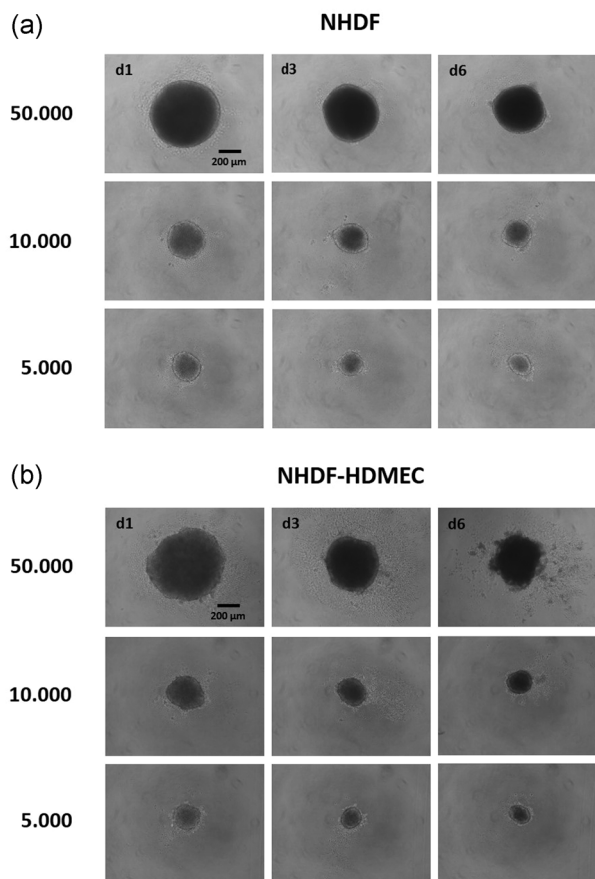


**FIGURE 2** Representative photomicrographs (phase contrast) showing the morphology of spheroids. (a) NHDF spheroid of all three sizes. For each size, the same spheroid was photo-documented on Days 1, 3, and 6. (b) NHDF-HDMEC spheroid of all three sizes. For each size, the same spheroid was photo-documented on Days 1, 3, and 6. HDMEC, human dermal microvascular endothelial cell; NHDF, normal human dermal fibroblasts

the coculture spheroids were surrounded by more cellular debris, which can clearly be seen for cocultures spheroids consisting of 50,000 cells on Day 3 and Day 6.

In line with our previously published results on the development of spheroid's size with differing cellular compositions (Metzger et al., 2011) the size of all spheroids under investigation continuously decreased over time (Figures 3a and 4a). The very small standard deviations presented in Figures 3a and 4a emphasize the performance of the LOT impressively.

### 3.2 | Success of dissociation into single cells

The proposed dissociation protocol allowed for a successful dissociation of mono- and coculture spheroids under standardized conditions. It was not necessary to vary these conditions in relation to the size or the age of the spheroids. All spheroids could be dissociated within 10 min under continuous shaking at 37°C in AccuMax supported by a subsequent pipetting procedure creating

shear forces. The success of the enzymatic dissociation was first checked microscopically, revealing only a few cellular aggregates, which could not be found after passing the cell suspension through the 70 µm-preseparation filters. In addition, no cellular aggregates could finally be found in the filters indicating, that all persisting aggregates could be loosened sufficiently. The LUNA FL cell counter allowed for the quantification of the number of single cells and revealed at least 95% single cells for all spheroids (Figures 4, 3b,c, and 4b,c). For NHDF, some differences between spheroids of different sizes were detectable: The NHDF spheroids consisting of 50,000 cells revealed a slightly lower amount of single cells on Day 1 and Day 3. Almost no influence on the amount of single cells could be found for the coculture spheroids (Figure 4b,c). The additional presentation of these results showing an alternative comparison in Figures 3c and 4c focuses on the influence of the age of spheroids. Of interest, an increase in the number of single cells could be detected for both, mono- and coculture spheroids, consisting of 50,000 cells. The direct comparison of the results obtained for mono- and coculture spheroids revealed a significantly reduced number of single cells for most of the coculture spheroids (50,000 cells on Day 3 and Day 6; 10,000 cells on Day 1, Day 3, and Day 6; 5000 cells on Day 3).

### 3.3 | Flow cytometric live-dead-assay and quantification of debris

For any downstream application of the cells, the viability of the cells after dissociation of the spheroids is extremely important. On the one hand, the incubation time in AccuMax is quite short (10 min), on the other hand, repeated centrifugation as well as the influence of the applied shear forces by stringent pipetting might lead to impaired viability of the cells. As shown in Figures 3d,e, and 4d,e, the viability of the cells after dissociation determined with the live-dead-assay in combination with flow cytometric quantification was between 85% and 95% in most cases. The lowest viability was detected for the coculture spheroids (10,000 cells) on Day 1 with 80.1%. Only slight differences for the comparison of the different spheroid sizes shown in Figures 3d and 4d could be seen. Furthermore, there is only a slight influence of the age of the spheroids on viability (Figures 3e and 4e). In some cases, a tendency of the highest number of viable cells on Day 3 can be seen, but the differences are only in part significant. However, the direct comparison between mono- and coculture spheroids revealed a strong influence of the chosen cell type on their viability after dissociation: For almost all groups, NHDF-HDMEC-coculture spheroids were significantly less viable than mono-culture spheroids. Only on Day 6, no difference could be seen for spheroids consisting of 5000 cells and 50,000 cells.

In line with these findings, the amount of cellular debris quantified by flow cytometry clearly increased for dissociated coculture spheroids on Day 3 and Day 6, whereas no increase in debris could be observed for NHDF-mono-culture spheroids (Figure 5). A direct

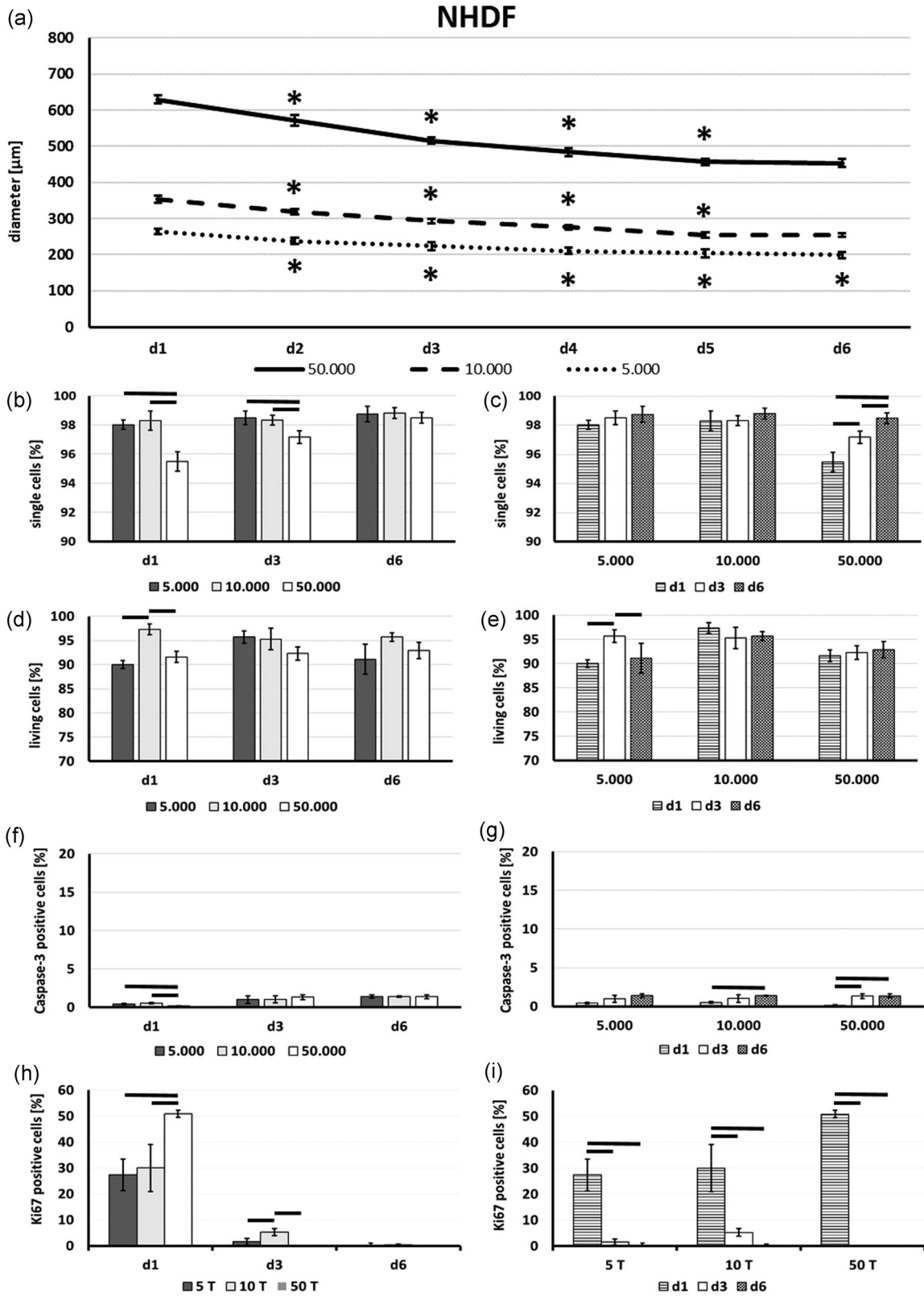


FIGURE 3 (See caption on next page)

comparison of the amount of debris between mono- and cocultures revealed significantly more debris for the cocultures on Day 3 and Day 6.

### 3.4 | Flow cytometric quantification of apoptotic cells

Figures 3f,g and 4f,g illustrate the results of the quantification of Caspase-3 positive cells by means of flow cytometry. At first glance, the low number of apoptotic NHDF for the dissociated mono-culture spheroids is obvious. Even on Day 6, the biggest spheroids exhibited less than 2% apoptotic cells. Of note, only a small increase in apoptotic cells over time could be detected (Figure 3f,g). In contrast, we found a quite high number of apoptotic cells for the coculture spheroids, reaching up to almost 18% (Figure 4f,g). For both dissociated mono- and coculture spheroids, the number of apoptotic cells is not influenced by the size of the spheroids (Figures 3f and 4f), but by the age of the spheroids, which can be impressively be seen for the coculture spheroids. In all cases, the number of apoptotic cells was higher in dissociated coculture-spheroids compared with the according mono-culture spheroids

### 3.5 | Flow cytometric quantification of proliferating cells

On Day 1 after generation, a surprisingly high number of Ki67 positive cells could be found in both, mono- and coculture spheroids (Figures 3h and 4h). Of interest, more cells were proliferative in both groups of spheroids consisting of 50,000 cells compared with the smaller spheroids. But already on Day 3 after generation, the high number of Ki67 positive cells dramatically decreased and almost no proliferation could be detected on Day 6 anymore (Figures 3i and 4i). In most cases, the number of Ki67 positive cells was significantly higher in mono-culture spheroids compared with coculture spheroids.

## 4 | DISCUSSION

It is widely accepted that spheroids are a promising cell culture model for many future applications. As no further stabilizing matrix is needed, they are better suitable to reflect the physiological situation

of cells in living tissues than traditional 2D-cell culture approaches with cells grown in monolayers on an artificial, mostly polystyrene surface. Furthermore, cells organized in spheroids can communicate with each other by intensive cell-cell contacts and with components of the extracellular matrix (ECM) within the spheroids. We have been using LOT for the generation of spheroids in several studies so far and are convinced by the performance of the method allowing the production of highly standardized spheroids of up to three types of cells (Metzger et al., 2011; Walser et al., 2013). Contrary to reports on the size development of tumor spheroids (Mamnoon et al., 2020), the size of spheroids of primary cells again decreased over time probably caused by a decrease in the size of single cells within the spheroid (Grässer et al., 2018; Takezawa et al., 1993). The loss of contact inhibition, which is characteristic of tumor cells, leads to high cell proliferation in tumor spheroids whereas only a low cellular proliferation is reported for primary cells organized as spheroids (Janjic et al., 2020).

For the analysis of spheroids, a multitude of techniques can be applied including quantitative real-time polymerase chain reaction, analysis of the proteome, or quantification of secreted growth factors, just to name a few. The quantification of specific parameters on a single cell basis by flow cytometry could be an ideal supplement to the aforementioned global tests and requires a single cell suspension with no cell aggregates. First, aggregates could lead to technical problems in the cytometer, for example, clogging of filters, nozzles, or tubes. Second, they might lead to misinterpretations of the results or to nonreproducible results. It is obvious, that the dissociation of spheroids is more challenging than dissociation of monolayers of cells due to the fact that the access of the enzyme solution is limited in 3D-aggregates. Furthermore, an optimal dissociation of spheroids must enable a complete dissociation into single cells and must not be harmful to the cells leading to impaired viability at the same time (Fischer et al., 2018). Recently, we were able to establish a dissociation protocol for mono- and coculture spheroids consisting of 10,000 or 50,000 NHDF and HDMEC, respectively (Grässer et al., 2018). In the aforementioned study, we used Accutase® for the dissociation of spheroids. Accutase® is a mixture of collagenolytic and proteolytic enzymes used for the detachment of adherent growing cells from the culture surface and is derived from *Crustacea*. It is supposed to be very gentle to the cells compared with trypsin by not affecting the surface epitopes, which is very important for subsequent flow cytometry analysis. However, it was not possible

**FIGURE 3** Characterization of NHDF mono-cultures before and after dissociation of spheroids. (a) Development of the size of spheroids as revealed by consecutive measurement of the diameter of 10 spheroids for each size and cellular composition. \* indicates significant differences compared with spheroids of the same size of the previous day,  $p < .05$ . (b, c) Amount of single cells after dissociation of spheroids as revealed by analysis with the LUNA FL Cell Counter ( $N = 4$ ). (d, e) Amount of living cells after dissociation of spheroids as revealed by FACS analysis of the live-dead-assay ( $N = 4$ ). (f, g) Amount of apoptotic cells after dissociation of spheroids as revealed by FACS analysis using the PE Active Caspase-3 Apoptosis Kit ( $N = 3$ ). (h, i) Amount of proliferating cells after dissociation of spheroids as revealed by FACS quantification of Ki67 positive cells ( $N = 3$ ). Two different comparisons of the results are shown in (b–i): The focus in (b, d, f, h) is on the influence of the size of spheroids, the focus in (c, e, g, i) is on the influence of age of the spheroids. Bars in (b–i) indicate significant differences within one group,  $p < .05$ . FACS, fluorescence-activated cell sorting; NHDF, normal human dermal fibroblasts

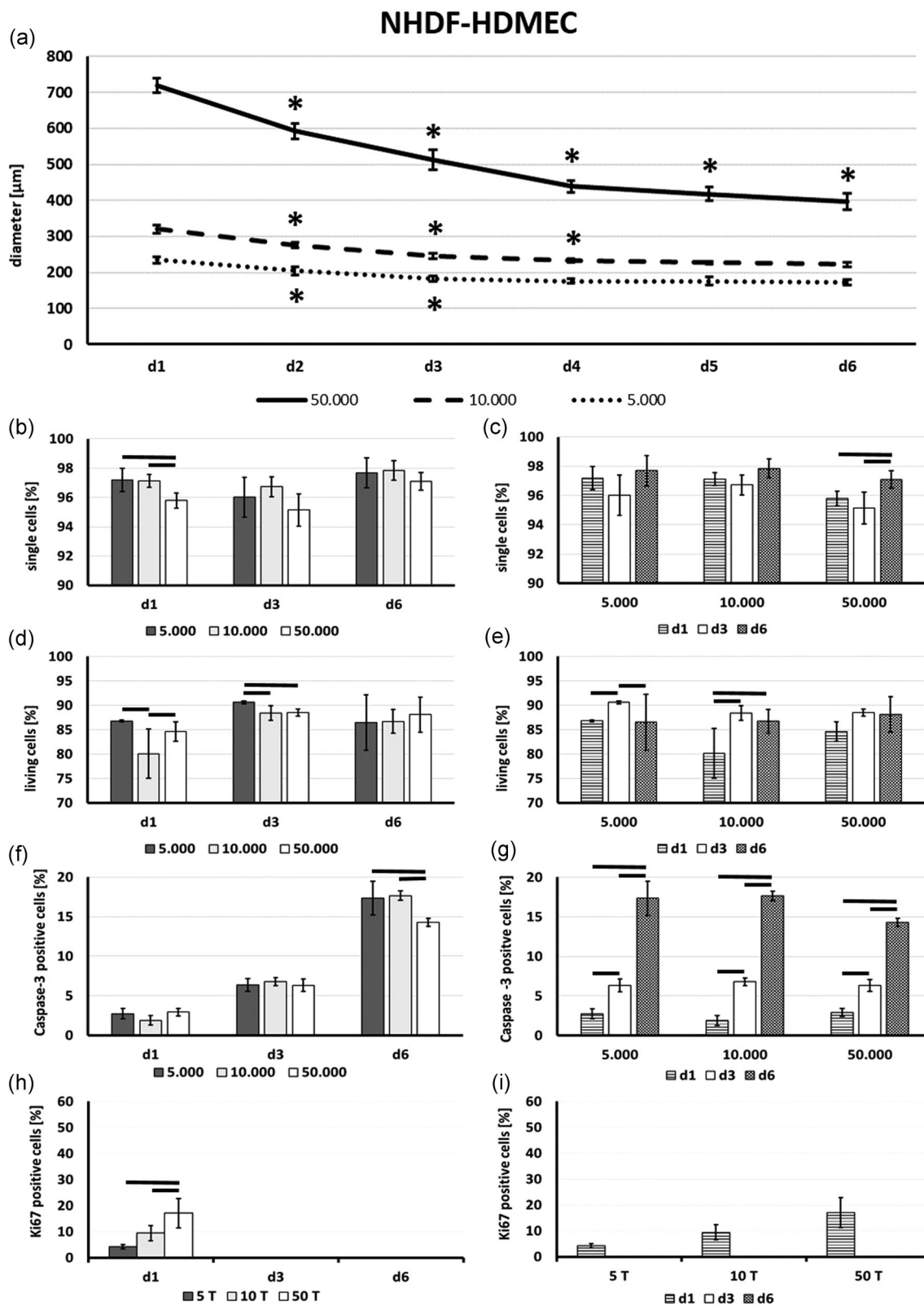


**FIGURE 4** (See caption on next page)



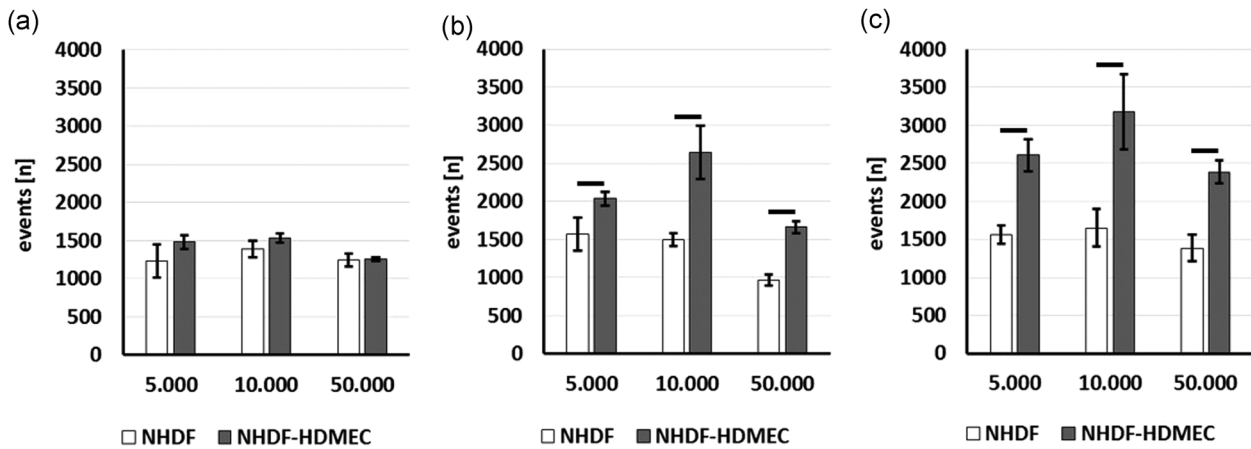


**FIGURE 5** Number of events gated as debris in single-cell suspensions after dissociation of spheroids. (a) Spheroids were dissociated on Day 1 after generation. (b) Spheroids were dissociated on Day 3 after generation. (c) Spheroids were dissociated on Day 6 after generation.  $N = 4$ , bars indicate significant differences within one group,  $p < .05$

to apply the same dissociation conditions for all spheroids under investigation. The bigger and the older the spheroids were, the more stringent dissociation conditions had to be chosen (Grässer et al., 2018). Furthermore, after dissociation of HDMEC mono-culture spheroids, the cells exhibited a very low cell recovery rate and a great number of dead cells, which further increased over time. This is in line with the results of another report from our group revealing a high number of apoptotic HDMEC in mono-culture spheroids (Walser et al., 2013). In consequence, only NHDF-HDMEC coculture spheroids and no HDMEC mono-culture spheroids were considered in the present study.

Using an alternative enzyme, we switched to the related and commercially available cell detachment solution AccuMax, which contains the same enzymes as Accutase®, but at an approximately threefold higher concentration. It turned out, that AccuMax was clearly superior compared with Accutase®: All spheroids could be successfully dissociated into single cells within 10 min and no additional use of collagenase was necessary. In all cases, the dissociation resulted in at least 95% of single cells and just a few small aggregates. In addition, we checked the pre-separation filters after centrifugation microscopically and did not find any big aggregates. Interestingly, the number of single cells increased for the mono- and coculture spheroids consisting of 50,000 cells, but not for the

spheroids consisting of 5,000 or 10,000 cells. One explanation could be a longer diffusion time for AccuMax to reach the central regions of the spheroids in combination with an increasing rate of apoptotic cells over time (Fischer et al., 2018).

Fortunately, the higher efficiency of our optimized dissociation protocol did not affect the viability of the cells in a negative way. In most cases, the viability of the cell suspension was in the range between 85% and 95%, which is comparable to the amount of viable cells after standard trypsinization in 2D-cell cultures ( $> 95\%$ , empirical value from our lab). Fischer and coworkers also performed a detailed study on the efficiency of different protocols to dissociate spheroids of human-induced pluripotent stem cells. They found papain to be the optimal dissociation solution with viability of 93.6%, which is in line with our results, but the time for complete dissociation was 30 min compared with 10 min in our protocol. Despite the long incubation time, the amount of single cells was only 74.8% in their study (Fischer et al., 2018). Of interest, they also found many cells stained with both Calcein AM and PI, as shown in Figure 1. We tried to reduce the number of double-stained cells (washing, replacement of PI with ethidium homodimer 1), but we did not succeed. Even when we stained one population with calcein AM and another population with PI separately and mixed them after washing, double-stained cells were measured. Obviously, PI can easily be transferred

**FIGURE 4** Characterization of NHDF-HDMEC cocultures before and after dissociation of spheroids. (a) Development of size of spheroids as revealed by consecutive measurement of the diameter of 10 spheroids for each size and cellular composition. \* indicates significant differences compared with spheroids of the same size of the previous day,  $p < .05$ . (b, c) Amount of single cells after dissociation of spheroids as revealed by analysis with the LUNA FL Cell Counter ( $N = 4$ ). (d, e) Amount of living cells after dissociation of spheroids as revealed by FACS analysis of the live-dead-assay ( $N = 4$ ). (f, g) Amount of apoptotic cells after dissociation of spheroids as revealed by FACS analysis using the PE Active Caspase-3 Apoptosis Kit ( $N = 3$ ). (h, i) Amount of proliferating cells after dissociation of spheroids as revealed by FACS quantification of Ki67 positive cells ( $N = 3$ ). Two different comparisons of the results are shown in (b–i): The focus in (b, d, f, h) is on the influence of the size of spheroids, the focus in (c, e, g, i) is on the influence of age of the spheroids. Bars in (b–i) indicate significant differences within one group,  $p < .05$ . HDMEC, human dermal microvascular endothelial cells; FACS, fluorescence-activated cell sorting; NHDF, normal human dermal fibroblasts

from one cell to the other and is able to penetrate cells with impaired membrane integrity while the uptaken calcein-AM can still be converted by cellular enzymes. This explanation is in line with the report of Liu and coworkers, who worked with calcein AM and ethidium homodimer 1 and observed a population of double-stained cells, too (Liu et al., 2012). Our results show that the viability of the cells was only slightly affected by the age and size of the spheroids but strongly affected by the used cell type.

The irregular morphology of the coculture spheroids and the higher amount of cellular debris support the hypothesis of a significant influence of the chosen cell type on the viability. The higher amount of cellular debris of NHDF-HDMEC spheroids could already be seen during the microscopic observation of the spheroids in the agarose-coated wells before the dissociation. The significant differences detected by gating of the debris in the flow cytometric analysis are in line with this information. Potential production of additional debris during the dissociation process cannot be excluded but it is very unlikely that this will reverse the observed differences between NHDF spheroids and NHDF-HDMEC-spheroids. The high overall viability of the cells indicates that the central region of the spheroids is not necrotic, which is contrary to the assumption of a necrotic core in tumor spheroids. First, tumor cells are highly proliferative and have a high demand for oxygen and nutrients. Second, it could be shown in spheroids of nonmalignant cells that the packing density decreases with increasing spheroid size leading to a better supply of the cells located in the inner region of the spheroids (Murphy et al., 2017).

The number of apoptotic cells clearly depends on the chosen cell type and was always higher for the NHDF-HDMEC spheroids. In particular, HDMEC organized as spheroids are very sensitive to apoptosis. In an earlier study, we found a high number of approx. 25% apoptotic HDMEC in 3 days old spheroids (50,000 cells), which could significantly be reduced by adding another cell type (Walser et al., 2013). In vivo, the endothelium is formed by a monolayer of endothelial cells (Campinho et al., 2020). Consequently, the 3D organization of endothelial cells might be an unphysiological situation for the cells, leading to a high number of apoptotic cells, which clearly increases with the age of the spheroids. In contrast, only very few NHDF were found to be positive for caspase-3 and no increase over time could be seen making them promising candidates for long-term experiments or tissue engineering approaches (Kim et al., 2020).

Of interest, we found many Ki67 positive cells in both, mono- and coculture spheroids on Day 1. In NHDF spheroids, 27%–50% of all cells were Ki67 positive. This result is comparable to other reports in the literature (Schwarz et al., 2013). Here, a rate of 40%–60% Ki67 positive cells was found in subconfluent 2D-cultures of primary fibroblasts. But already 3 days after generation of the spheroids, a tremendous decrease in Ki67 positive cells could be seen. Granato et al. (2017) quantified the number of Ki67 positive cells by immunofluorescence staining of spheroid sections and found them only on Day 1 but not more on Day 3. All cells in the spheroid were resting cells in the G0-phase. Obviously, the cells in the 1-day-old spheroids did not adapt to the 3D-arrangement

representing a confluent culture in all three dimensions yet, resulting in high numbers of Ki67 positive cells which is comparable to the situation found in subconfluent 2D-cultures. However, already on Day 3, the proliferation marker is downregulated to more physiological rates found in healthy tissues. For example, in healthy myometrium, only 1.6% of all cells were found to be Ki67 positive (Eulálio Filho et al., 2019). In conclusion, spheroids are more suitable for reflecting the situation of cells in tissues better than 2D-cultures.

## 5 | CONCLUSIONS

The optimized dissociation protocol presented here is clearly superior compared with our previously published method: We were able to dissociate both, mono- and cocultures independent from their size and age with just one standardized dissociation protocol, resulting in an amount of at least 95% of single cells. The resulting cell suspensions were suitable to perform FACS analysis successfully. The rate of apoptotic cells was clearly influenced by the cell type and not by age or size. On Day 3 after generation, the number of proliferating cells in spheroids is comparable with the proliferation rate in healthy tissue.

## ACKNOWLEDGMENT

Open Access funding enabled and organized by Projekt DEAL.

## CONFLICT OF INTERESTS

The authors declare that there are no conflict of interests.

## AUTHOR CONTRIBUTIONS

Tim Pohlemann and Wolfgang Metzger conceived the study. Wolfgang Metzger, Barbara Rösch, Daniela Sossong, and Monika Bubel performed all the experiments. Wolfgang Metzger, Barbara Rösch, Daniela Sossong, and Monika Bubel discussed the results and Wolfgang Metzger prepared the first draft of the manuscript. All authors read, corrected, and approved the final manuscript.

## DATA AVAILABILITY STATEMENT

Data available on request from the authors

## ORCID

Wolfgang Metzger  <http://orcid.org/0000-0001-9668-4694>

## REFERENCES

- Achilli, T. M., Meyer, J., & Morgan, J. R. (2012). Advances in the formation, use and understanding of multi-cellular spheroids. *Expert Opinion on Biological Therapy*, 12, 1347–1360.
- Arufe, M. C., De la Fuente, A., Fuentes-Boquete, I., De Toro, F. J., & Blanco, F. J. (2009). Differentiation of synovial CD-105(+) human mesenchymal stem cells into chondrocyte-like cells through spheroid formation. *Journal of Cellular Biochemistry*, 108, 145–155.
- Benmeridja, L., De Moor, L., De Maere, E., Vanlauwe, F., Ryx, M., Tytgat, I., Vercruyse, C., Dubrue, P., Van Vlierberghe, S., Blondeel, P., & Declercq, H. (2020). High-throughput fabrication of vascularized adipose microtissues for 3D bioprinting. *Journal of Tissue Engineering and Regenerative Medicine*, 14, 840–854.

- Campinho, P., Vilfan, A., & Vermot, J. (2020). Blood flow forces in shaping the vascular system: A focus on endothelial cell behavior. *Frontiers in Physiology*, 11, 552.
- Cesarz, Z., & Tamama, K. (2016). Spheroid culture of mesenchymal stem cells. *Stem Cells International*, 2016, 9176357.
- Dorst, N., Oberringer, M., Grasser, U., Pohlemann, T., & Metzger, W. (2014). Analysis of cellular composition of co-culture spheroids. *Annals of Anatomy*, 196, 303–311.
- Eulálio Filho, W., Soares, E., Lima, M., Brazil, E., Rodrigues, R., Zeron, R., Silva, B. B., & Costa, P. (2019). Evaluation of KI-67 expression in uterine leiomyoma and in healthy myometrium: A pilot study. *Revista da Associação Médica Brasileira*, 65, 1459–1463.
- Fischer, B., Meier, A., Dehne, A., Salhotra, A., Tran, T. A., Neumann, S., Schmidt, K., Meiser, L., Neubauer, J. C., Zimmermann, H., & Gentile, L. (2018). A complete workflow for the differentiation and the dissociation of hiPSC-derived cardiospheres. *Stem Cell Research*, 32, 65–72.
- Foty, R. A., & Steinberg, M. S. (2005). The differential adhesion hypothesis: A direct evaluation. *Developmental Biology*, 278, 255–263.
- Friedrich, J., Ebner, R., & Kunz-Schughart, L. A. (2007). Experimental anti-tumor therapy in 3-D: Spheroids-old hat or new challenge? *International Journal of Radiation Biology*, 83, 849–871.
- Granato, G., Ruocco, M. R., Iaccarino, A., Masone, S., Cali, G., Avagliano, A., Russo, V., Bellevicine, C., Di Spigna, G., Fiume, G., Montagnani, S., & Arcucci, A. (2017). Generation and analysis of spheroids from human primary skin myofibroblasts: An experimental system to study myofibroblasts deactivation. *Cell Death Discovery*, 3, 17038.
- Grässer, U., Bubel, M., Sossong, D., Oberringer, M., Pohlemann, T., & Metzger, W. (2018). Dissociation of mono- and co-culture spheroids into single cells for subsequent flow cytometric analysis. *Annals of Anatomy*, 216, 1–8.
- Heiss, M., Hellström, M., Kalén, M., May, T., Weber, H., Hecker, M., Augustin, H. G., & Korff, T. (2015). Endothelial cell spheroids as a versatile tool to study angiogenesis in vitro. *FASEB Journal*, 29, 3076–3084.
- Hirschhaeuser, F., Menne, H., Dittfeld, C., West, J., Mueller-Klieser, W., & Kunz-Schughart, L. A. (2009). Multicellular tumor spheroids: An underestimated tool is catching up again. *Journal of Biotechnology*, 148, 3–15.
- Janjic, K., Schadl, B., Andrukhov, O., & Agis, H. (2020). The response of gingiva monolayer, spheroid, and ex vivo tissue cultures to collagen membranes and bone substitute. *Journal of Tissue Engineering and Regenerative Medicine*, 14, 1307–1317.
- Kim, S. J., Kim, E. M., Yamamoto, M., Park, H., & Shin, H. (2020). Engineering multi-cellular spheroids for tissue engineering and regenerative medicine. *Advanced Healthcare Material*, 9, e2000608.
- Laschke, M. W., Schank, T. E., Scheuer, C., Kleer, S., Schuler, S., Metzger, W., Eglin, D., Alini, M., & Menger, M. D. (2013). Three-dimensional spheroids of adipose-derived mesenchymal stem cells are potent initiators of blood vessel formation in porous polyurethane scaffolds. *Acta Biomaterialia*, 9, 6876–6884.
- Lazzari, G., Nicolas, V., Matsusaki, M., Akashi, M., Couvreur, P., & Mura, S. (2018). Multicellular spheroid based on a triple co-culture: A novel 3D model to mimic pancreatic tumor complexity. *Acta Biomaterialia*, 78, 296–307.
- Lazzari, G., Vinciguerra, D., Balasso, A., Nicolas, V., Goudin, N., Garfa-Traore, M., Fehér, A., Dinnyés, A., Nicolas, J., Couvreur, P., & Mura, S. (2019). Light sheet fluorescence microscopy versus confocal microscopy: In quest of a suitable tool to assess drug and nanomedicine penetration into multicellular tumor spheroids. *European Journal of Pharmaceutics and Biopharmaceutics: Official Journal of Arbeitsgemeinschaft für Pharmazeutische Verfahrenstechnik e.V.*, 142, 195–203.
- Liu, S., Zhang, Q. S., Hester, W., O'Brien, M. J., Savoie, F. H., & You, Z. (2012). Hyaluronan protects bovine articular chondrocytes against cell death induced by bupivacaine at supraphysiologic temperatures. *American Journal of Sports Medicine*, 40, 1375–1383.
- Mamnoon, B., Feng, L., Froberg, J., Choi, Y., Venkatachalem, S., & Mallik, S. (2020). Hypoxia-responsive, polymeric nanocarriers for targeted drug delivery to estrogen receptor-positive breast cancer cell spheroids. *Molecular Pharmaceutics*, 17, 4312–4322.
- Meier-Hubbertain, J. C., & Sanderson, M. P. (2019). Establishment and analysis of a 3D co-culture spheroid model of pancreatic adenocarcinoma for application in drug discovery. *Methods in Molecular Biology*, 1953, 163–179.
- Metzger, W., Rother, S., Pohlemann, T., Moller, S., Schnabelrauch, M., Hintze, V., & Scharnweber, D. (2017). Evaluation of cell-surface interaction using a 3D spheroid cell culture model on artificial extracellular matrices. *Material Science and Engineering C*, 73, 310–318.
- Metzger, W., Schimmelpfennig, L., Schwab, B., Sossong, D., Dorst, N., Bubel, M., Görg, A., Pütz, N., Wennemuth, G., Pohlemann, T., & Oberringer, M. (2013). Expansion and differentiation of human primary osteoblasts in two- and three-dimensional culture. *Biotechnic & Histochemistry*, 88, 86–102.
- Metzger, W., Sossong, D., Bachle, A., Putz, N., Wennemuth, G., Pohlemann, T., & Oberringer, M. (2011). The liquid overlay technique is the key to formation of co-culture spheroids consisting of primary osteoblasts, fibroblasts and endothelial cells. *Cytotherapy*, 13, 1000–1012.
- Murphy, K. C., Hung, B. P., Browne-Bourne, S., Zhou, D., Yeung, J., Genetos, D. C., & Leach, J. K. (2017). Measurement of oxygen tension within mesenchymal stem cell spheroids. *Journal of the Royal Society, Interface*, 14, 20160851.
- Nimmerjahn, A., Kirchhoff, F., Kerr, J. N., & Helmchen, F. (2004). Sulforhodamine 101 as a specific marker of astroglia in the neocortex in vivo. *Nature Methods*, 1, 31–37.
- Schwarz, F., Jennewein, M., Bubel, M., Holstein, J. H., Pohlemann, T., & Oberringer, M. (2013). Soft tissue fibroblasts from well healing and chronic human wounds show different rates of myofibroblasts in vitro. *Molecular Biology Reports*, 40, 1721–1733.
- Steinberg, M. S. (1970). Does differential adhesion govern self-assembly processes in histogenesis? Equilibrium configurations and the emergence of a hierarchy among populations of embryonic cells. *Journal of Experimental Zoology*, 173, 395–433.
- Takezawa, T., Mori, Y., Yonaha, T., & Yoshizato, K. (1993). Characterization of morphology and cellular metabolism during the spheroid formation by fibroblasts. *Experimental Cell Research*, 208, 430–441.
- Unger, C., Kramer, N., Walzl, A., Scherzer, M., Hengstschlager, M., & Dolznig, H. (2014). Modeling human carcinomas: Physiologically relevant 3D models to improve anti-cancer drug development. *Advanced Drug Delivery Reviews*, 79–80, 50–67.
- Walser, R., Metzger, W., Görg, A., Pohlemann, T., Menger, M. D., & Laschke, M. W. (2013). Generation of co-culture spheroids as vascularisation units for bone tissue engineering. *European Cells & Materials*, 26, 222–233.
- Wang, W., Itaka, K., Ohba, S., Nishiyama, N., Chung, U. I., Yamasaki, Y., & Kataoka, K. (2009). 3D spheroid culture system on micropatterned substrates for improved differentiation efficiency of multipotent mesenchymal stem cells. *Biomaterials*, 30, 2705–2715.

**How to cite this article:** Metzger, W., Rösch, B., Sossong, D., Bubel, M., & Pohlemann, T. (2021). Flow cytometric quantification of apoptotic and proliferating cells applying an improved method for dissociation of spheroids. *Cell Biol Int*, 45, 1633–1643. <https://doi.org/10.1002/cbin.11618>